

## $\Delta$ -excitations and the three-nucleon force

E. Epelbaum,<sup>1,2,\*</sup> H. Krebs,<sup>2,†</sup> and Ulf-G. Meißner<sup>2,1,‡</sup>

<sup>1</sup>*Forschungszentrum Jülich, Institut für Kernphysik (Theorie), D-52425 Jülich, Germany*

<sup>2</sup>*Universität Bonn, Helmholtz-Institut für Strahlen- und Kernphysik (Theorie), D-53115 Bonn, Germany*

(Dated: February 13, 2013)

We study the three-nucleon force in chiral effective field theory with explicit  $\Delta$ -resonance degrees of freedom. We show that up to next-to-next-to-leading order, the only contribution to the isospin symmetric three-nucleon force involving the spin-3/2 degrees of freedom is given by the two-pion-exchange diagram with an intermediate delta, frequently called the Fujita-Miyazawa force. We also analyze the leading isospin-breaking corrections due to the delta. For that, we give the first quantitative analysis of the delta quartet mass splittings in chiral effective field theory including the leading electromagnetic corrections. The charge-symmetry breaking three-nucleon force due to an intermediate delta excitation is small, of the order of a few keV.

PACS numbers: 13.75.Cs, 21.30.-x

### I. INTRODUCTION AND SUMMARY

The importance of the  $\Delta$ -excitation in the three-nucleon force (3NF) has been already realized fifty years ago by Fujita and Miyazawa in their seminal work [1]. Their paper has been the seed for many meson-theoretical approaches to the 3NF like the families of Tucson-Melbourne [2, 3], Brazilian [4] or Urbana-Illinois [5, 6] 3NFs, see the review article [7] and the recent general introduction [8]. Nowadays, the appropriate tool to analyze the forces between nucleons is chiral effective field theory, a program started by Weinberg [9]. There has been quite a sizeable body of further work on the structure of 3NFs within the framework of EFT, with appropriate references given below. Still, in the EFT with explicit deltas most investigations so far have considered the effects based on the leading pion-nucleon-delta coupling. In this work, we want to go one step further. In the two-nucleon system, we had already considered the effects of subleading  $\pi N\Delta$  couplings on the description of the peripheral phase shifts [11]. Such effects appear at next-to-next-to-leading order (NNLO) in the Weinberg counting. It is therefore appropriate to extend these considerations to the 3NF, more precisely to the  $\Delta$ -contributions to the isospin-symmetric 3NF at NNLO and the leading isospin-breaking corrections to the 3NF. An important ingredient in latter type of forces stems from the mass splittings in the quartet of  $\Delta$ -states ( $\Delta^{++}, \Delta^+, \Delta^0, \Delta^-$ ). These splittings receive contributions from the strong and electromagnetic interactions, thus one needs to consider an appropriate extension of the power counting including the explicit soft and hard photon effects.

The pertinent results of this investigation can be summarized as follows:

- i) We have evaluated the  $\Delta$ -contributions to the three-nucleon force up to NNLO and shown that the only non-vanishing topology is the two-pion exchange diagram with an intermediate delta resonance, commonly called the Fujita-Miyazawa force. This implies that the leading contributions to the  $1\pi$ - $4N$ -contact and the  $6N$ -nucleon contact topologies are not saturated by the  $\Delta$ .
- ii) We have compared the  $2\pi$ -exchange 3NF in the EFT with and without explicit  $\Delta$  degrees of freedom. We show that these representations lead to comparable results for the strength of the 3NF if the same data basis for pion-nucleon scattering is used to pin down the LECs in the two versions of the theory, see table I.

---

\*Email: e.epelbaum@fz-juelich.de

†Email: hkrebs@itkp.uni-bonn.de

‡Email: meissner@itkp.uni-bonn.de; URL: [www.itkp.uni-bonn.de/~meissner/](http://www.itkp.uni-bonn.de/~meissner/)

- iii) We have analyzed for the first time the mass splitting in the delta quartet from strong and electromagnetic contributions with EFT up-to-and-including second chiral order. Note that chiral extrapolation formulae for the strong splitting have already been given earlier in Ref. [12]. The delta mass splittings are parameterized in terms of two independent parameters, cf. Eq. (3.7). These can only be determined with large uncertainties since the available information on the various delta masses is fairly scarce and uncertain, see tables II,III.
- iv) We have shown how the proton-neutron mass difference can be eliminated from the delta-full EFT by field redefinitions, extending the method developed in [25]. This facilitates the calculation of the isospin-breaking effects to the 3NF considerably.
- v) We have worked out the leading isospin-breaking contributions to the 3NF due to an intermediate  $\Delta$ -excitation, see Fig. 1. The leading charge-symmetry conserving and charge-symmetry breaking contributions to the 3NF are given in Eq. (3.24) in momentum space. We also give the coordinate space representation. We estimate the contribution from the charge-symmetry breaking force to the 3N binding energy to be of the order of a few keV.

The manuscript is organized as follows. In sec. II we investigate the delta contributions to the 3NF up-to-and-including next-to-next-to-leading order in the so-called small scale expansion (SSE) [10]. The calculation of the leading isospin-violating contributions is presented in sec. III. As a first step, we analyze the mass splittings within the delta quartet and calculate the strong and electromagnetic contributions to the various particles, see sec. III A. In sec. III B we discuss field redefinitions to eliminate the proton-to-neutron mass shift from the effective Lagrangian which considerably simplifies the calculation of the isospin-breaking effects. The isospin-breaking 3NFs due to explicit deltas are then worked out in sec. III C.

## II. $\Delta$ -CONTRIBUTIONS TO THE THREE-NUCLEON FORCE UP TO NNLO

Our calculations are based on Weinberg's power counting [9] utilizing the small scale expansion [10]. In this framework, irreducible diagrams with two or more nucleons which give rise to the nuclear forces are ordered according to the power  $\nu$  of the expansion parameter  $Q/\Lambda$ , where  $Q$  collectively denotes small pion four-momenta, the pion mass, baryon three-momenta and the nucleon-delta mass splitting and  $\Lambda$  is the pertinent hard scale. For an irreducible  $N$ -nucleon diagram, the power  $\nu$  is given by:

$$\nu = -2 + 2N + 2(L - C) + \sum_i V_i \Delta_i. \quad (2.1)$$

Here,  $L$ ,  $C$  and  $V_i$  refer to the number of loops, separately connected pieces and vertices of type  $i$ , respectively. Further, the vertex dimension  $\Delta_i$  is given by

$$\Delta_i = d_i + \frac{1}{2}b_i - 2, \quad (2.2)$$

where  $b_i$  is the number of baryon field operators and  $d_i$  is the number of derivative, insertions of  $M_\pi$  and/or the delta-nucleon mass splitting,  $\Delta \equiv m_\Delta - m_N$ .<sup>1</sup>

For the calculation of the isospin-conserving three-nucleon force (3NF) up to NNLO we use the effective chiral Lagrangian already given in [11]. The only additional terms that need to be considered are the leading-order  $NN \rightarrow N\Delta$  and  $N\Delta \rightarrow NN$  contact interactions

$$\bar{T}_i^\mu N \bar{N} S_\mu \tau^i N + \text{h. c.}, \quad (2.3)$$

where  $N$  denotes the large component of the nucleon field,  $T_i^\mu$  is the large component of the delta field, with  $i$  an isospin and  $\mu$  a Lorentz index. Furthermore,  $\tau^i$  and  $S_\mu$  are Pauli isospin matrices and  $S_\mu$  denotes the covariant spin vector. For more details on the notation and the effective Lagrangian the reader is referred to [13]. The contact

---

<sup>1</sup> Notice that we use the symbol  $\Delta$  for both the spin-3/2 field and the  $N\Delta$  mass splitting. It is, however, always evident from the context what is meant.

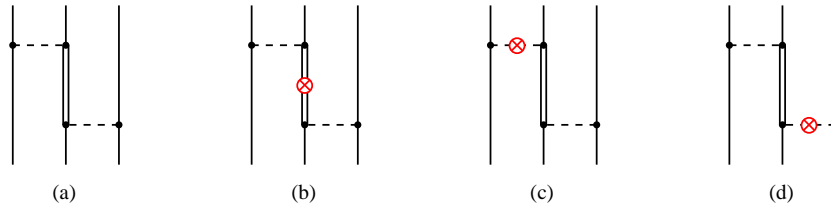


FIG. 1: Leading isospin-conserving (diagram (a)) and isospin-breaking (diagrams (b-d)) contributions to the 3NF with a  $\Delta$ -excitation. Solid, dashed and double lines represent nucleons, pions and deltas, respectively. Solid dots denote the leading isospin-invariant vertices, crossed circles are the isospin-breaking vertices from the  $SU(2)_V$ -rotated effective Lagrangian as explained in section III A.

interactions in Eq. (2.3) were already considered by van Kolck [14] who worked out the corresponding contributions to the 3NF. As pointed out in Ref. [15], matrix elements of the resulting 3NFs between antisymmetrized  $|NNN\rangle$  states vanish, see also [16] for a related discussion. The reason for vanishing of these 3NF contributions can be understood already at the level of the effective Lagrangian. To that aim, let us rewrite Eq. (2.3) including the spin and isospin 3/2 projectors  $P_{\mu\nu}^{3/2}$  and  $\xi_{ij}^{3/2}$  explicitly:

$$\bar{T}_i^\mu N \bar{N} S_\mu \tau^i N = \bar{T}_j^\nu \xi_{ji}^{3/2} P_{\nu\mu}^{3/2} N \bar{N} S^\mu \tau^i N, \quad (2.4)$$

with

$$\xi_{ij}^{3/2} = \frac{2}{3}\delta_{ij} - \frac{i}{3}\epsilon_{ijk}\tau^k, \quad P_{\mu\nu}^{3/2} = g_{\mu\nu} - v_\mu v_\nu - \frac{4}{1-d}S_\mu S_\nu. \quad (2.5)$$

Here,  $v_\mu$  denotes the baryon four-velocity and  $d$  the number of space-time dimensions. In four dimensions with  $v = (1, 0, 0, 0)$ , the spin 3/2 projector reduces to

$$P_{ij}^{3/2} = -\left[\frac{2}{3}\delta_{ij} - \frac{i}{3}\epsilon_{ijk}\sigma^k\right], \quad (2.6)$$

with  $\sigma^k$  denoting the Pauli spin matrices. It is straightforward to see that the antisymmetrized Feynman rules for the particular contact interactions vanish:

$$\xi_{ij}^{3/2}(1)P_{kl}^{3/2}(1)\tau_2^j\sigma_2^l\mathcal{A}_{12} = \xi_{ij}^{3/2}(2)P_{kl}^{3/2}(2)\tau_1^j\sigma_1^l\mathcal{A}_{12} = 0, \quad (2.7)$$

where the subscripts of the Pauli spin and isospin matrices refer to the nucleon labels and the antisymmetrization operator for momentum-independent interactions  $\mathcal{A}_{12}$  has the form

$$\mathcal{A}_{12} = \frac{1 - P_{12}}{2}, \quad \text{with} \quad P_{12} = \frac{1 + \vec{\sigma}_1 \cdot \vec{\sigma}_2}{2} \frac{1 + \tau_1 \cdot \tau_2}{2}. \quad (2.8)$$

The labeled projector operators  $\xi_{ij}^{3/2}(X)$  and  $P_{ij}^{3/2}(X)$  in Eq. (2.7) are defined according to

$$\xi_{ij}^{3/2}(X) = \frac{2}{3}\delta_{ij} - \frac{i}{3}\epsilon_{ijk}\tau_X^k, \quad P_{ij}^{3/2}(X) = -\left[\frac{2}{3}\delta_{ij} - \frac{i}{3}\epsilon_{ijk}\sigma_X^k\right], \quad X \in \{1, 2\}. \quad (2.9)$$

We are now in the position to discuss the 3NF contributions due to intermediate  $\Delta$  excitations. Due to vanishing of the lowest-order contact interaction, the complete effect due the  $\Delta$  is given by a single two-pion ( $2\pi$ ) exchange diagram (a) in Fig. 1. It is well known that the corresponding 3NF contribution is exactly reproduced at NNLO in EFT without explicit  $\Delta$ -fields via resonance saturation of the low-energy constants (LECs)  $c_{3,4}$  accompanying the subleading  $\pi\pi NN$  vertices [17]:  $c_3 = -2c_4 = -4h_A^2/(9\Delta)$ . Here,  $h_A$  denotes the leading  $\Delta N\pi$  axial-vector coupling constant.

Let us now regard the NNLO contributions. First, we emphasize that there are still no diagrams involving contact interactions at this order. In fact, since  $NNN\Delta$  contact interactions contain at least two derivatives, they start to

	$Q^3$ , no $\Delta$	$Q^2$ with $\Delta$ , fit 1	$Q^2$ with $\Delta$ , fit 2	$Q^3$ with $\Delta$ , fits 1,2
$a$	-0.70	0	0	-0.70
$b$	-2.34	-1.70	-1.03	-2.18
$d$	-0.89	-0.42	-0.26	-0.83

TABLE I: Values of the coefficients  $a$ ,  $b$  and  $d$  entering the  $2\pi$ -exchange 3NF in Eq. (2.11) in units of  $M_\pi^{-1}$  for  $a$  and  $M_\pi^{-3}$  for  $b$  and  $d$ .

contribute to the 3NF only at N<sup>3</sup>LO. Therefore, the only diagrams which need to be considered are the ones which result from graph (a) in Fig. 1 by substituting one of the leading  $\pi N\Delta$  vertices by the subleading one which is proportional to the combination of LECs ( $b_3 + b_8$ ), see Refs. [11, 13].<sup>2</sup> Since this vertex involves a time derivative, the corresponding 3NF contribution is shifted to higher orders due to the  $1/m_N$ -suppression. We, therefore, end up with the conclusion that the  $2\pi$ -exchange 3NF from diagram (a) in Fig. 1 represents the only additional contribution which arises in EFT with explicit  $\Delta$  up to NNLO.

Before ending this section, it is interesting to compare the strength of various pieces in the  $2\pi$ -exchange 3NF in EFT with and without explicit  $\Delta$  degrees of freedom which has the form

$$V_{2\pi} = \sum_{i \neq j \neq k} \frac{1}{2} \left( \frac{g_A}{2F_\pi} \right)^2 \frac{\vec{\sigma}_i \cdot \vec{q}_i \vec{\sigma}_j \cdot \vec{q}_j}{[q_i^2 + M_\pi^2][q_j^2 + M_\pi^2]} F_k^{\alpha\beta} \tau_i^\alpha \tau_j^\beta, \quad (2.10)$$

where  $\vec{q}_i \equiv \vec{p}_i' - \vec{p}_i$ ;  $\vec{p}_i$  ( $\vec{p}_i'$ ) is the initial (final) momentum of the nucleon  $i$  and

$$F_k^{\alpha\beta} = \delta^{\alpha\beta} [-a + b \vec{q}_i \cdot \vec{q}_j - c(q_i^2 + q_j^2)] - d \epsilon^{\alpha\beta\gamma} \tau_k^\gamma \vec{q}_i \times \vec{q}_j \cdot \vec{\sigma}_k. \quad (2.11)$$

The coefficients  $a$ ,  $b$  and  $d$  can be expressed in terms of various LECs while  $c = 0$ , see Ref. [18] for more details. In EFT without explicit  $\Delta$ , the chiral expansion for these coefficients starts at NNLO (i.e. at order  $Q^3$ ) where one has:

$$a^{(3)} = \frac{4c_1 M_\pi^2}{F_\pi^2}, \quad b^{(3)} = \frac{2c_3}{F_\pi^2}, \quad d^{(3)} = -\frac{c_4}{F_\pi^2}. \quad (2.12)$$

Here the superscripts refer to the chiral order. In EFT with explicit  $\Delta$  fields, the dominant contributions arise already at NLO

$$a^{(2)} = 0, \quad b^{(2)} = -\frac{8h_A^2}{9\Delta F_\pi^2}, \quad d^{(2)} = -\frac{2h_A^2}{9\Delta F_\pi^2}, \quad (2.13)$$

with the corrections at order  $Q^3$  being still given by Eq. (2.12). In Table I, we compare the values for the coefficients  $a$ ,  $b$  and  $d$  in the theory with and without explicit  $\Delta$  based on our determination [11] of the LECs  $c_i$  and  $b_3 + b_8$ . We remind the reader that fits 1 and 2 are based on the different values for the  $\pi N\Delta$  coupling constant  $h_A$  used as an input: the SU(4)/large- $N_c$  value  $h_A = 3g_A/(2\sqrt{2}) = 1.34$  in fit 1 versus  $h_A = 1.05$  [13] in fit 2. Clearly, at NLO this uncertainty in the value of  $h_A$  directly transforms into the uncertainty in the coefficients  $b$  and  $d$ , see the third and fourth columns in Table I. At NNLO, however, both fits 1 and 2 lead to very similar results for the S- and P-wave  $\pi N$  threshold parameters [11] and, consequently, for the coefficients  $b$  and  $d$ . A similar observation is also made for the subleading  $2\pi$ -exchange NN potential in Ref. [11]. Another interesting result is that both EFTs with and without  $\Delta$  lead to very similar values for the coefficients  $a$ ,  $b$  and  $d$  at NNLO. This seems to contradict the conclusion of Ref. [19] where a significant overestimation of the  $\Delta$ -contribution to the coefficients  $b$  and  $d$  by about 25% was found in EFT without explicit  $\Delta$  fields. As shown in Table I, the coefficients  $b$  and  $d$  are indeed overestimated in the  $\Delta$ -less theory, but only by about 7%. There are several reasons for this difference. First, our results for  $b$  and  $d$  involve contributions beyond the ones generated by the  $\Delta$  excitation. Secondly, we also take into account the subleading  $\Delta$ -contribution governed by the  $b_3 + b_8$ -vertex from  $\mathcal{L}_{\pi N\Delta}^{(2)}$  which is not considered in Ref. [19]. Switching off the  $b_3 + b_8$ -interaction, however, tend to further decrease the above mentioned overestimation and can, therefore, not explain the discrepancy.

<sup>2</sup> Due to parity invariance, the subleading  $\pi NN$  vertices contain two derivatives or one insertion of  $M_\pi^2$  more than the leading one and thus need not be considered at NNLO.

The most important difference between our work and the one of Ref. [19] concerns the determination of the LECs  $c_3$  and  $c_4$ . In [19], this was achieved via matching the P-wave  $\pi N$  threshold parameters for  $j = 3/2$ ,  $a_{1+}^+$  and  $a_{1+}^-$ . This leads to values for  $b$  and  $d$  which are quoted in Eq. (15) of that work. On the other hand, in [11] we used not only the  $j = 3/2$  but also the  $j = 1/2$  P-wave parameters  $a_{1-}^+$  and  $a_{1-}^-$  as well as the S-wave coefficients  $a_{0+}^+$  and  $b_{0+}^+$  to pin down the LECs  $c_i$  and  $b_3 + b_8$ . This turns out to be the main reason for the observed difference.

### III. LEADING ISOSPIN-BREAKING EFFECTS

Our next goal is to study the leading isospin-breaking contributions to the 3NF. This can be done following the lines of Refs. [20, 21] where we worked out the leading and subleading isospin-breaking 2N and 3N potentials, see also Refs. [22, 23, 24, 25] for a related work on this subject. Here and in what follows, we adopt the same counting rules for the electric charge  $e$  and the quark mass ratio  $\epsilon = (m_u - m_d)/(m_u + m_d) \sim -1/3$  as in Refs. [20, 21], namely

$$\epsilon \sim e \sim \frac{Q}{\Lambda}; \quad \frac{e^2}{(4\pi)^2} \sim \frac{Q^4}{\Lambda^4}. \quad (3.1)$$

The leading isospin-breaking vertices have the dimension  $\Delta_i = 2$  and correspond to the charged-to-neutral pion and proton-to-neutron mass differences [20] and, as will be shown below, mass splittings between the different charge states of the  $\Delta$ . It is easy to verify using Eqs. (2.1) and (2.2) that the dominant isospin-breaking 3NF which involves an intermediate delta excitation results at order  $\nu = 4$  from isospin-breaking pion-, nucleon- and delta-mass insertions in the first diagram in Fig. 1. Notice that the leading isospin-breaking  $\pi\pi NN$  vertex of dimension  $\Delta_i = 2$  also generates the 3NF contribution at order  $\nu = 4$  [21, 24] which, however, does not involve  $\Delta$ -excitations and is, therefore, irrelevant for the present study. Thus, in order to proceed with the calculation of the leading isospin-breaking 3NF contributions due to intermediate  $\Delta$ -excitations, we first need to analyze the delta mass splittings in chiral effective field theory.

#### A. Delta mass splittings in chiral effective field theory

To analyze the delta mass splitting in chiral effective field theory, we need to include hard virtual photons in the effective pion-nucleon-delta Lagrangian. Specifically, we are interested in the leading-order virtual photon effects that show up as local operators of dimension  $\Delta_i = 3$ . To construct these terms, we employ the standard spurion method, see e.g. [26, 27, 28, 29]. The resulting Lagrangian reads

$$\begin{aligned} \mathcal{L}_{\Delta\gamma}^{\Delta_i=3} = & -\bar{T}_i^\mu F_\pi^2 \left[ f_1^\Delta \delta_{ij} \langle Q_+^2 - Q_-^2 \rangle + f_2^\Delta \delta_{ij} \langle Q_+ \rangle Q_+ + f_3^\Delta \delta_{ij} \langle Q_+ \rangle^2 \right. \\ & \left. + f_4^\Delta \langle \tau^i Q_+ \rangle \langle \tau^j Q_+ \rangle + f_5^\Delta \langle \tau^i Q_- \rangle \langle \tau^j Q_- \rangle \right] g_{\mu\nu} T_j^\nu \end{aligned} \quad (3.2)$$

where  $\langle \dots \rangle$  denotes the isospin trace, the  $Q_\pm$  are defined as in [27] and  $F_\pi$  is the pion decay constant in the chiral limit. The factor  $F_\pi^2$  ensures that the LECs  $f_i^\Delta$  have the same dimension as the corresponding strong LECs [27]. Notice that while all couplings and masses appearing in the effective Lagrangian should, strictly speaking, be taken at their chiral limit values, to the accuracy we are working, we can use their pertinent physical values. We further emphasize that the expected natural size of the LECs  $f_i^\Delta$  is

$$F_\pi^2 f_i^\Delta \sim M_\rho \frac{1}{(4\pi)^2}, \quad (3.3)$$

so that, according to Eqs. (2.2) and (3.1), the corresponding vertices are indeed of the dimension  $\Delta_i = 3$ . The electromagnetic mass term of the delta is readily deduced from Eq. (3.2) by considering the terms without pion fields, e.g.

$$\mathcal{L}_{\Delta\gamma, \text{mass}}^{\Delta_i=3} = -F_\pi^2 \bar{T}_i^\mu \left[ (f_1^\Delta + f_3^\Delta) e^2 \delta_{ij} + f_2^\Delta \frac{e^2}{2} (1 + \tau^3) \delta_{ij} + f_4^\Delta e^2 \delta_{i3} \delta_{j3} \right] g_{\mu\nu} T_j^\nu. \quad (3.4)$$

Note that the first term in this equation leads to an overall mass shift in the delta quartet, while the other two contribute to various splittings. The relevant isospin conserving and strong isospin violating terms at leading order are given by [10]

$$\mathcal{L}_{\Delta IV}^{\Delta_i=2} = -\bar{T}_i^\mu c_5^\Delta (\chi_+ - \langle \chi_+ \rangle) \delta_{ij} g_{\mu\nu} T_j^\nu = -\bar{T}_i^\mu c_5^\Delta 2M_\pi^2 \varepsilon \tau^3 \delta_{ij} g_{\mu\nu} T_j^\nu + \dots \quad (3.5)$$

where ellipses refer to terms which contain pion fields. Note that in Ref. [10] the LEC  $c_5^\Delta$  was denoted as  $a_5$ . Combining Eqs. (3.4) and (3.5), we arrive at the leading strong and electromagnetic isospin-breaking contributions to the delta mass term

$$\mathcal{L}_{\Delta, \text{mass}, IV} = -\bar{T}_i^\mu \left[ -\delta m_\Delta^1 \frac{1}{2} \tau^3 \delta_{ij} - \delta m_\Delta^2 \frac{3}{4} \delta_{i3} \delta_{j3} \right] g_{\mu\nu} T_j^\nu, \quad (3.6)$$

with

$$\begin{aligned} \delta m_\Delta^1 &= -4M_\pi^2 \varepsilon c_5^\Delta - F_\pi^2 e^2 f_2^\Delta, \\ \delta m_\Delta^2 &= -\frac{4}{3} F_\pi^2 e^2 f_4^\Delta. \end{aligned} \quad (3.7)$$

Notice that according to the counting rules in Eq. (3.1), the dominant term in Eq. (3.6) arises from strong isospin breaking while the leading electromagnetic contribution is shifted one order higher. At least in the nucleon sector, this pattern is in a reasonable agreement with the data and the strong shift gives indeed numerically the dominant contribution. Since we are interested here only in the leading isospin-breaking effects due to explicit  $\Delta$  degrees of freedom, it is, strictly speaking, sufficient to keep only the strong delta mass shift. We will, however, keep both the leading strong and electromagnetic delta mass shifts in what follows and thus generate a portion of the subleading isospin-breaking contributions to the 3NF. At the order we are working, isospin-breaking contribution to the delta self-energy results from the tree diagram with a single insertion from Eq. (3.6). The delta mass splittings can, therefore, be directly read off from Eq. (3.6). Switching from the Rarita-Schwinger representation to physical delta fields ( $\Delta^{++}$ ,  $\Delta^+$ ,  $\Delta^0$ ,  $\Delta^-$ ) one obtains:

$$\begin{aligned} m_{\Delta^{++}} &= \tilde{m}_\Delta + \frac{1}{2} \delta m_\Delta^1, \\ m_{\Delta^+} &= \tilde{m}_\Delta + \frac{1}{6} \delta m_\Delta^1 + \frac{1}{2} \delta m_\Delta^2, \\ m_{\Delta^0} &= \tilde{m}_\Delta - \frac{1}{6} \delta m_\Delta^1 + \frac{1}{2} \delta m_\Delta^2, \\ m_{\Delta^-} &= \tilde{m}_\Delta - \frac{1}{2} \delta m_\Delta^1. \end{aligned} \quad (3.8)$$

Notice that the isospin-invariant delta mass shift  $\delta m_\Delta$ , defined according to  $\tilde{m}_\Delta = \overset{\circ}{m}_\Delta + \delta m_\Delta$ , can, in principle, be extracted using the chiral limit of the  $N\Delta$  splitting  $\Delta_0 \simeq 330$  MeV from Ref. [30] and the value of the nucleon mass in the chiral limit  $\overset{\circ}{m}_N \simeq 890$  MeV from Ref. [31]. This leads to  $\overset{\circ}{m}_\Delta \simeq 1220$  MeV. We further emphasize that in the absence of electromagnetic corrections (no  $\delta m_\Delta^2$ -term), there is an equal spacing between the members of the quartet. In that case, one has  $\tilde{m}_\Delta = \overset{\circ}{m}_\Delta$  and all splittings are equal to  $\delta m_\Delta^1/3$ . We also recover the SU(6) results  $m_{\Delta^{++}} - m_{\Delta^-} = 3(m_{\Delta^+} - m_{\Delta^0})$  independent of the strength of the electromagnetic LEC  $f_4^\Delta$ , see e.g. [32]. Our results for the strong splittings are, of course, in agreement with the ones of Ref. [12]. In that paper, higher order corrections were also evaluated with particular emphasis on the quark mass dependence of the delta splittings to be used as chiral extrapolation functions in lattice gauge theory.

To further analyze the delta mass splittings, we need input values for some of these masses. Astonishingly, the available information of these masses is fairly scarce and uncertain, see e.g. the most recent listings of the particle data group [33]. From pion-nucleon scattering, one can extract  $m_{\Delta^{++}}$  and  $m_{\Delta^0}$  as well as the average delta mass  $\tilde{m}_\Delta$

$$\tilde{m}_\Delta \equiv \frac{1}{4} (m_{\Delta^{++}} + m_{\Delta^+} + m_{\Delta^0} + m_{\Delta^-}) = \tilde{m}_\Delta + \frac{1}{4} \delta m_\Delta^2. \quad (3.9)$$

The values for the Breit-Wigner masses  $m_{\Delta^{++}}$  and  $m_{\Delta^0}$  quoted in Ref. [33] and based on the determinations from Refs. [34, 35, 36, 37] are all in a reasonable agreement with each other (within the given error bars). The only exception is the analysis of Ref. [38], which yields significantly different values for  $m_{\Delta^{++}}$  and  $m_{\Delta^0}$  (but has also the largest error bars). From photoproduction reactions, one can, in principle, determine the mass of  $\Delta^+$ . The two

available results for  $\Delta^+$  quoted in [33] differ, however, significantly from each other. We, therefore, refrain from using  $m_{\Delta^+}$  in our study. Finally, no experimental information is available for  $m_{\Delta^-}$ . To pin down the values for  $\tilde{m}_\Delta$ ,  $\delta m_\Delta^1$  and  $\delta m_\Delta^2$  we proceed in two different ways. First, we use as an input the available data on  $m_{\Delta^{++}}$ ,  $m_{\Delta^0}$  (except the values from Ref. [38]) and the average delta mass  $\tilde{m}_\Delta$ . For the latter, we adopt the value  $\tilde{m}_\Delta = 1233$  MeV which is consistent with the estimation of Ref. [33],  $\tilde{m}_\Delta = 1231 \dots 1233$  MeV as well as with the most recent determination from Ref. [39],  $\tilde{m}_\Delta = 1233.4 \pm 0.4$  MeV. This leads to

$$\tilde{m}_\Delta = 1233.4 \pm 0.7 \text{ MeV}, \quad \delta m_\Delta^1 = -5.3 \pm 2.0 \text{ MeV}, \quad \delta m_\Delta^2 = -1.7 \pm 2.7 \text{ MeV}, \quad (3.10)$$

where the error bars result from using different input values for  $m_{\Delta^{++}}$  and  $m_{\Delta^0}$ , see Table II. Notice that the

$\tilde{m}_\Delta$	$\delta m_\Delta^1$	$\delta m_\Delta^2$	$m_{\Delta^{++}}$	$m_{\Delta^+}$	$m_{\Delta^0}$	$m_{\Delta^-}$	input
1233.63	-6.15	-2.50	1230.55*	1231.35	1233.40*	1236.70	[34]
1234.10	-7.20	-4.40	1230.50*	1230.70	1233.10*	1237.70	[35]
1233.15	-4.50	-0.60	1230.90*	1232.10	1233.60*	1235.40	[36]
1232.75	-3.30	1.00	1231.10*	1232.70	1233.80*	1234.40	[37]

TABLE II: Delta masses and LECs for various input values of  $m_{\Delta^{++}}$  and  $m_{\Delta^0}$  as indicated by the star. Additional input is the average delta mass  $\tilde{m}_\Delta = 1233$  MeV. All values are given in units of MeV.

obtained results for  $\delta m_\Delta^1$  and  $\delta m_\Delta^2$  are of a natural size. Indeed, based on the naive dimensional analysis, one expects  $|\delta m_\Delta^1| \sim |\epsilon M_\pi^2/M_\rho| \simeq 8$  MeV and  $|\delta m_\Delta^2| \sim e^2 M_\rho/(4\pi)^2 \simeq 1.5$  MeV.

As an alternative, one can use in the determination of  $\tilde{m}_\Delta$ ,  $\delta m_\Delta^1$  and  $\delta m_\Delta^2$  the quark model relation [32]

$$m_{\Delta^+} - m_{\Delta^0} = m_p - m_n \quad (3.11)$$

instead of the average delta mass  $\tilde{m}_\Delta$ . This fixes the value of  $\delta m_\Delta^1$  and leads to less uncertain results for  $\tilde{m}_\Delta$  and  $\delta m_\Delta^2$ , see Table III for more details:

$\tilde{m}_\Delta$	$\delta m_\Delta^2$	$m_{\Delta^{++}}$	$m_{\Delta^+}$	$m_{\Delta^0}$	$m_{\Delta^-}$	$\tilde{m}_\Delta$	input
1232.49	0.53	1230.55*	1232.11	1233.40*	1234.43	1232.62	[34]
1232.44	0.03	1230.50*	1231.81	1233.10*	1234.38	1232.45	[35]
1232.84	0.23	1230.90*	1232.31	1233.60*	1234.78	1232.90	[36]
1233.04	0.23	1231.10*	1232.51	1233.80*	1234.98	1233.10	[37]

TABLE III: Delta masses and LECs for various input values of  $m_{\Delta^{++}}$  and  $m_{\Delta^0}$  as indicated by the star. Additional input is the quark model relation (3.11). All values are given in units of MeV.

$$\tilde{m}_\Delta = 1232.7 \pm 0.3 \text{ MeV}, \quad \delta m_\Delta^1 = -3.9 \text{ MeV}, \quad \delta m_\Delta^2 = 0.3 \pm 0.3 \text{ MeV}. \quad (3.12)$$

It is comforting to see that the results of both determinations are compatible with each other. In particular, the value obtained for the average delta mass,  $\tilde{m}_\Delta = 1232.45 \dots 1233.10$  MeV, agrees with both the estimation of Ref. [33] and the determination of Ref. [39]. We further emphasize that the LECs  $c_5^\Delta$  and  $f_2^\Delta$  can be deduced from  $\delta m_N^{\text{str}}$  and  $\delta m_N^{\text{em}}$  if one uses the relation (3.11) separately for the strong and electromagnetic mass shifts. Using  $\delta m_N^{\text{str}} \equiv (m_p - m_n)^{\text{str}} = -2.05 \pm 0.3$  MeV and  $\delta m_N^{\text{em}} \equiv (m_p - m_n)^{\text{em}} = 0.76 \pm 0.3$  MeV from Ref. [40], see also [41] for a recent determination from lattice QCD, one obtains  $c_5^\Delta = 3c_5 = -0.24 \pm 0.04$  GeV $^{-1}$  and  $f_2^\Delta = 3f_2 = -2.9 \pm 1.1$  GeV $^{-1}$ , where  $c_5$  and  $f_2$  are the corresponding LECs in the nucleon sector.

## B. Field redefinitions and the proton-to-neutron mass shift

Having worked out the delta mass splitting in chiral EFT, it is, in principle, a straightforward task to calculate the dominant isospin-breaking 3NF contribution due to explicit  $\Delta$  following the line of Ref. [20]. The calculations may be facilitated if one eliminates the nucleon mass shift from the effective Lagrangian. This allows to get rid of diagrams which involve reducible topologies and, therefore, enables to use the Feynman graph technique to derive

the 3NF. As already demonstrated in Ref. [25] for EFT without explicit  $\Delta$ , the proton-to-neutron mass difference can be eliminated from  $\mathcal{L}_{\text{eff}}$  via a suitable redefinition of the pion and nucleon fields (or, equivalently, via a suitable *local*  $SU(2)_V$  transformation) in favor of new vertices proportional to  $\delta m_N$ . This approach can be straightforwardly generalized to include the  $\Delta$  as an explicit degree of freedom. To be specific, consider the effective chiral Lagrangian  $\mathcal{L}_{\text{eff}}(\Phi, J)$ , where  $\Phi \equiv \{U, \bar{N}, N, \bar{T}, T\}$  ( $J \equiv \{r_\mu, l_\mu, s, p\}$ ) collectively denote the pion, nucleon and delta fields (right- and left-handed, scalar and pseudoscalar external sources). The effective Lagrangian  $\mathcal{L}_{\text{eff}}(\Phi, J)$  is invariant under local chiral rotations  $G = SU(2)_L \times SU(2)_R$ :

$$\mathcal{L}_{\text{eff}}(\Phi, J) \xrightarrow{g \in G} \mathcal{L}_{\text{eff}}(\Phi', J') \equiv \mathcal{L}_{\text{eff}}(g(\Phi), g(J)) = \mathcal{L}_{\text{eff}}(\Phi, J). \quad (3.13)$$

For the purpose of computing S-matrix elements in the few-nucleon sector, the external sources can be set to zero from the beginning (with the exception of the scalar source that is equal to the quark mass matrix in this limit). In the absence of external sources, the effective Lagrangian  $\mathcal{L}_{\text{eff}}(\Phi) \equiv \mathcal{L}_{\text{eff}}(\Phi, J)|_{J=0}$  is only invariant under global chiral rotations. Local chiral transformations  $g \in G$  will, in general, affect its form

$$\mathcal{L}_{\text{eff}}(\Phi) \xrightarrow{g \in G} \mathcal{L}_{\text{eff}}(g(\Phi)) = \mathcal{L}_{\text{eff}}(\Phi) + \delta \mathcal{L}_{\text{eff}}(\Phi), \quad (3.14)$$

and obviously may be viewed as a redefinition of fields  $\Phi$ . The task is now to choose the transformation  $V$  in such a way that the resulting correction  $\delta \mathcal{L}_{\text{eff}}(\Phi)$  eliminates the nucleon mass shift term

$$-\bar{N} \delta m_N \frac{1}{2} \tau^3 N, \quad \delta m_N = -4 c_5 \epsilon M_\pi^2 - e^2 F_\pi^2 f_2, \quad (3.15)$$

in  $\mathcal{L}_{\text{eff}}(\Phi)$ . Notice that in practice, it is more convenient to compute the correction  $\delta \mathcal{L}_{\text{eff}}$  applying the inverse rotation to the external currents

$$\mathcal{L}_{\text{eff}}(g(\Phi)) = \mathcal{L}_{\text{eff}}(\Phi, g^{-1}(J)) \Big|_{J=0} = \mathcal{L}_{\text{eff}}(\Phi) + \delta \mathcal{L}_{\text{eff}}(\Phi). \quad (3.16)$$

Following Ref. [25], we choose the local  $SU(2)_V$  transformation such that

$$r'_\mu = V r_\mu V^\dagger + i V \partial_\mu V^\dagger, \quad l'_\mu = V l_\mu V^\dagger + i V \partial_\mu V^\dagger, \quad s' = V s V^\dagger, \quad p' = V p V^\dagger \quad (3.17)$$

with  $V = \exp(i v \cdot x \delta m_N \tau^3 / 2)$ . Notice that as pointed out in Ref. [25], this transformation does not lead to explicitly  $x$ -dependent vertices since the interactions in  $\mathcal{L}_{\text{eff}}$  conserve electric charge. One obtains for the chiral vielbein  $u_\mu = i [u^\dagger (\partial_\mu - i r_\mu) u - u (\partial_\mu - i l_\mu) u^\dagger]$  and connection  $\Gamma_\mu = 1/2 [u^\dagger (\partial_\mu - i r_\mu) u + u (\partial_\mu - i l_\mu) u^\dagger]$

$$\begin{aligned} u_\mu \Big|_{J=0} &\rightarrow i (u^\dagger (\partial_\mu - i r'_\mu) u - u (\partial_\mu - i l'_\mu) u^\dagger) \Big|_{J=0} = u_\mu \Big|_{J=0} + \frac{\delta m_N}{2} v_\mu (u^\dagger \tau^3 u - u \tau^3 u^\dagger) \\ &= u_\mu \Big|_{J=0} + \frac{\delta m_N}{F_\pi} v_\mu [\boldsymbol{\tau} \times \boldsymbol{\pi}]_3 + \mathcal{O}(\boldsymbol{\pi}^3), \\ \Gamma_\mu \Big|_{J=0} &\rightarrow \frac{1}{2} (u^\dagger (\partial_\mu - i r'_\mu) u + u (\partial_\mu - i l'_\mu) u^\dagger) \Big|_{J=0} = \Gamma_\mu \Big|_{J=0} - i \frac{\delta m_N}{4} v_\mu (u^\dagger \tau^3 u + u \tau^3 u^\dagger) \\ &= \Gamma_\mu \Big|_{J=0} - i \frac{\delta m_N}{2} v_\mu \tau^3 + i \frac{\delta m_N}{4 F_\pi^2} v_\mu [\boldsymbol{\pi}^2 \tau^3 - \boldsymbol{\pi} \cdot \boldsymbol{\tau} \pi_3] + \mathcal{O}(\boldsymbol{\pi}^4), \end{aligned} \quad (3.18)$$

and, consequently, for the nucleon and delta kinetic energy terms:

$$\begin{aligned} \bar{N} i v \cdot D N &= \bar{N} (i v \cdot \partial + i v \cdot \Gamma) N \rightarrow \bar{N} \left( i v \cdot \partial + \frac{\delta m_N}{2} \tau^3 + \mathcal{O}(\boldsymbol{\pi}^2) \right) N, \\ -\bar{T}_i^\mu (i v \cdot D_{ij}) g_{\mu\nu} T_j^\nu &= -\bar{T}_i^\mu (i (v \cdot \partial + v \cdot \Gamma) \delta_{ij} + \epsilon_{ijk} \langle \tau^k v \cdot \Gamma \rangle) g_{\mu\nu} T_j^\nu \\ &\rightarrow -\bar{T}_i^\mu \left( \left( i v \cdot \partial + \frac{3\delta m_N}{2} \tau^3 \right) \delta_{ij} + \mathcal{O}(\boldsymbol{\pi}^2) \right) g_{\mu\nu} T_j^\nu. \end{aligned} \quad (3.19)$$

Here we have used the following identity for the Rarita-Schwinger field:

$$\bar{T}_i^\mu \epsilon_{ijk} T_j^\nu = i \bar{T}_i^\mu \delta_{ij} \tau^k T_j^\nu. \quad (3.20)$$

Thus, we finally end up with the modification of the lowest-order effective Lagrangian

$$\begin{aligned} \mathcal{L}_{\text{eff}}^{\Delta_i=0} &\rightarrow \mathcal{L}_{\text{eff}}^{\Delta_i=0} - \delta m_N [(v \cdot \partial \boldsymbol{\pi}) \times \boldsymbol{\pi}]_3 + \frac{1}{2} (\delta m_N)^2 (\boldsymbol{\pi}^2 - \pi_3 \pi_3) + \mathcal{O}(\boldsymbol{\pi}^4) + \frac{\delta m_N}{2} \bar{N} (\tau^3 + \mathcal{O}(\boldsymbol{\pi}^2)) N \\ &\quad - \frac{3\delta m_N}{2} \bar{T}_i^\mu (\tau^3 \delta_{ij} + \mathcal{O}(\boldsymbol{\pi}^2)) g_{\mu\nu} T_j^\mu. \end{aligned} \quad (3.21)$$

For the pion and pion-nucleon sectors, these results agree with the ones obtained in Ref. [25].

Finally, we would like to emphasize that although the applied field redefinition is, strictly speaking, of a more general type than the one discussed in [42, 43], it is straightforward to show that both  $\mathcal{L}_{\text{eff}}$  and  $\mathcal{L}_{\text{eff}} + \delta\mathcal{L}_{\text{eff}}$  lead to the same  $S$ -matrix elements in the few-nucleon sector. The corresponding Green functions in the original and modified theories are, however, not the same<sup>3</sup> and related to each other by the transformations  $V$ :

$$\frac{\delta^{2n} Z[J, \eta, \bar{\eta}]}{\delta\eta_{j_1}(x_1) \dots \delta\eta_{j_n}(x_n) \delta\bar{\eta}_{l_1}(y_1) \dots \delta\bar{\eta}_{l_n}(y_n)} \Big|_{J=\eta=\bar{\eta}=0} = \sum_{k_1, l_1, \dots, k_n, l_n} \frac{\delta^{2n} Z[J', \eta', \bar{\eta}']}{\delta\eta'_{k_1}(x_1) \dots \delta\eta'_{k_n}(x_n) \delta\bar{\eta}'_{l_1}(y_1) \dots \delta\bar{\eta}'_{l_n}(y_n)} \Big|_{J'=\eta'=\bar{\eta}'=0} \times V_{k_1, j_1}(x_1) \dots V_{k_n, j_n}(x_n) V_{l_1, l_1}^\dagger(y_1) \dots V_{l_n, l_n}^\dagger(y_n). \quad (3.22)$$

Here  $Z[J, \eta, \bar{\eta}]$  is the generating functional

$$e^{iZ[J, \eta, \bar{\eta}]} = \int [D\Phi] e^{i \int d^4x [\mathcal{L}_{\text{eff}}(\Phi, J) + \bar{\eta}N + \bar{N}\eta]}, \quad (3.23)$$

and  $\eta' = V\eta$ ,  $\bar{\eta}' = \bar{\eta}V^\dagger$ .

### C. Isospin-breaking 3NFs due to explicit deltas

We are now in the position to present our results for the leading isospin-breaking contributions to the 3NF due to an intermediate  $\Delta$ -excitation. A straightforward evaluation of Feynman diagrams (b-d) in Fig. 1 yields the following charge-symmetry conserving (CSC), i.e. class-II in the notation of Ref. [21], and charge-symmetry breaking (CSB), i.e. class-III, contributions to the 3NF:

$$\begin{aligned} V_{3N}^{\text{Class-II}} &= - \sum_{i \neq j \neq k} \frac{g_A^2 h_A^2}{18F_\pi^4 \Delta} \frac{\vec{q}_i \cdot \vec{\sigma}_i \vec{q}_k \cdot \vec{\sigma}_k}{[q_i^2 + M_\pi^2][q_k^2 + M_\pi^2]} \left( \tau_i^3 \tau_k^3 \left( \frac{4\delta M_\pi^2}{q_k^2 + M_\pi^2} - \frac{3\delta m_\Delta^2}{4\Delta} \right) \vec{q}_i \cdot \vec{q}_k \right. \\ &\quad \left. + \left( \frac{\delta M_\pi^2}{q_k^2 + M_\pi^2} [\boldsymbol{\tau}_i \times \boldsymbol{\tau}_j]^3 \tau_k^3 - \frac{3\delta m_\Delta^2}{8\Delta} [\boldsymbol{\tau}_i \times \boldsymbol{\tau}_k]^3 \tau_j^3 \right) [\vec{q}_i \times \vec{q}_k] \cdot \vec{\sigma}_j \right), \\ V_{3N}^{\text{Class-III}} &= - \sum_{i \neq j \neq k} \frac{g_A^2 h_A^2 (\delta m_\Delta^1 - 3\delta m_N)}{216F_\pi^4 \Delta^2} \frac{\vec{q}_i \cdot \vec{\sigma}_i \vec{q}_k \cdot \vec{\sigma}_k}{[q_i^2 + M_\pi^2][q_k^2 + M_\pi^2]} \left( 5 [\boldsymbol{\tau}_i \times \boldsymbol{\tau}_k]^3 [\vec{q}_i \times \vec{q}_k] \cdot \vec{\sigma}_j \right. \\ &\quad \left. + 4(\boldsymbol{\tau}_j \cdot \boldsymbol{\tau}_k \tau_i^3 - 2\boldsymbol{\tau}_i \cdot \boldsymbol{\tau}_k \tau_j^3) \vec{q}_i \cdot \vec{q}_k \right). \end{aligned} \quad (3.24)$$

The above expressions together with Eqs. (46), (49), (52) and (54) of Ref. [21] corresponding to the contributions from  $2\pi$ -exchange diagrams without intermediate delta-excitation provide the leading isospin-breaking 3NF in EFT with explicit  $\Delta$ .

The obtained results can be straightforwardly transformed into configuration space:

$$\begin{aligned} V_{3N}^{\text{Class-II}} &= - \sum_{i \neq j \neq k} \frac{g_A^2 h_A^2 M_\pi^6}{288\pi^2 F_\pi^4 \Delta} \vec{\sigma}_i \cdot \vec{\nabla}_{ij} \vec{\sigma}_k \cdot \vec{\nabla}_{kj} \left[ \tau_i^3 \tau_k^3 \vec{\nabla}_{ij} \cdot \vec{\nabla}_{kj} \left( \frac{2\delta M_\pi^2}{M_\pi^2} U_1(x_{ij}) U_2(x_{kj}) - \frac{3\delta m_\Delta^2}{4\Delta} U_1(x_{ij}) U_1(x_{kj}) \right) \right. \\ &\quad \left. + [\vec{\nabla}_{ij} \times \vec{\nabla}_{kj}] \cdot \vec{\sigma}_j \left( \frac{\delta M_\pi^2}{2M_\pi^2} [\boldsymbol{\tau}_i \times \boldsymbol{\tau}_j]^3 \tau_k^3 U_1(x_{ij}) U_2(x_{kj}) - \frac{3\delta m_\Delta^2}{8\Delta} [\boldsymbol{\tau}_i \times \boldsymbol{\tau}_k]^3 \tau_j^3 U_1(x_{ij}) U_1(x_{kj}) \right) \right], \\ V_{3N}^{\text{Class-III}} &= - \sum_{i \neq j \neq k} \frac{g_A^2 h_A^2 (\delta m_\Delta^1 - 3\delta m_N) M_\pi^6}{3456\pi^2 F_\pi^4 \Delta^2} \vec{\sigma}_i \cdot \vec{\nabla}_{ij} \vec{\sigma}_k \cdot \vec{\nabla}_{kj} \left[ 5 [\boldsymbol{\tau}_i \times \boldsymbol{\tau}_k]^3 [\vec{\nabla}_{ij} \times \vec{\nabla}_{kj}] \cdot \vec{\sigma}_j \right. \\ &\quad \left. + 4(\boldsymbol{\tau}_j \cdot \boldsymbol{\tau}_k \tau_i^3 - 2\boldsymbol{\tau}_i \cdot \boldsymbol{\tau}_k \tau_j^3) \vec{\nabla}_{ij} \cdot \vec{\nabla}_{kj} \right] U_1(x_{ij}) U_1(x_{kj}), \end{aligned} \quad (3.25)$$

<sup>3</sup> For example, the free nucleon propagator in the modified theory does not contain  $\delta m_N$  any more.

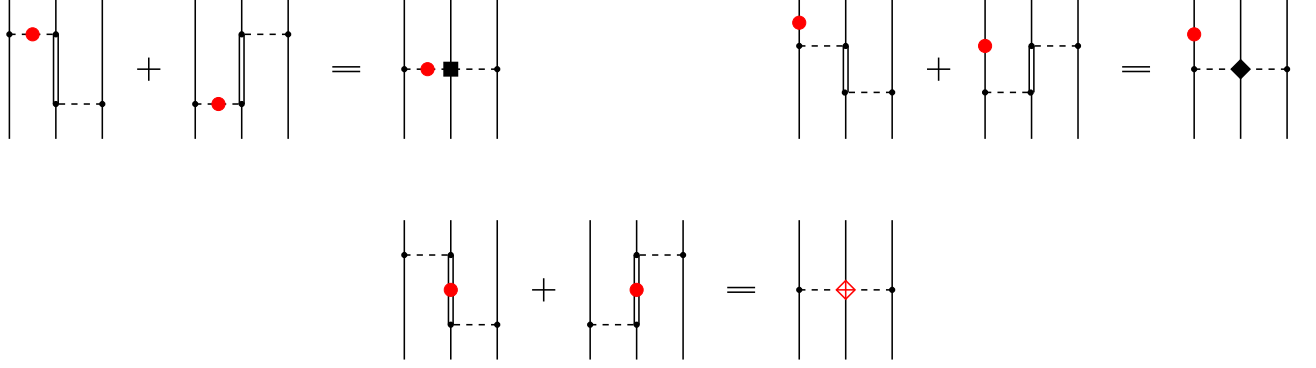


FIG. 2: Diagrams in the  $\Delta$ -less EFT which reproduce the  $\Delta$ -contributions to the leading isospin-breaking 3NF via resonance saturation of the LECs. Filled circles denote isospin-breaking pion, nucleon and delta mass shifts. Filled square and diamond refer to isospin-conserving vertices of dimension  $\Delta_i = 1$  and  $\Delta_i = 2$ . Crossed diamond denotes isospin-breaking strong and electromagnetic vertices of dimensions  $\Delta_i = 4$  and  $\Delta_i = 5$ , respectively. For diagrams involving the insertion of the nucleon mass shift, only two representative graphs are shown.

where  $\vec{r}_{ij} \equiv \vec{r}_i - \vec{r}_j$  is the distance between the nucleons  $i$  and  $j$ ,  $\vec{x}_i \equiv M_\pi \vec{r}_i$ ,  $\vec{\nabla}_i$  act on  $\vec{x}_i$  and  $x_{ij} \equiv |\vec{x}_{ij}|$ . Further, we have introduced the profile functions

$$\begin{aligned}
 U_1(x) &= \frac{4\pi}{M_\pi} \int \frac{d^3q}{(2\pi)^3} \frac{e^{i\vec{q}\cdot\vec{x}/M_\pi}}{q^2 + M_\pi^2} = \frac{e^{-x}}{x}, \\
 U_2(x) &= 8\pi M_\pi \int \frac{d^3q}{(2\pi)^3} \frac{e^{i\vec{q}\cdot\vec{x}/M_\pi}}{[q^2 + M_\pi^2]^2} = e^{-x}.
 \end{aligned} \tag{3.26}$$

It is instructive to understand how the obtained 3NF contributions are reproduced in EFT without explicit deltas. The trivial  $\Delta^{-1}$ - and  $\Delta^{-2}$ -dependence of the 3NF on the delta-nucleon mass splitting arising from the static propagator of the delta which enters Feynman diagrams (b-d) in Fig. 1 ensures that the results are reproduced in the  $\Delta$ -less theory by a *finite* number of higher-order graphs (via resonance saturation of certain LECs). This is depicted in Fig. 2. Here, we have switched back to the original Lagrangian with the nucleon mass shift which is more convenient to discuss resonance saturation. It should, however, be understood that for Feynman diagrams involving the nucleon mass shift, only irreducible contributions are taken into account. Consider first the CSC 3NF proportional to  $\delta M_\pi^2$  in Eq. (3.24). As expected, this contribution is exactly reproduced in the  $\Delta$ -less theory by an appropriate shift in the LECs  $c_3$  and  $c_4$  [17],  $c_3 = -2c_4 = -4h_A^2/(9\Delta)$ , which in this case is the subleading<sup>4</sup> effect (i.e. order  $\nu = 5$ ). The remaining terms in Eq. (3.24) are proportional to  $\Delta^{-2}$  which means that they arise in the  $\Delta$ -less theory only at sub-subleading order  $\nu = 6$ . This is consistent with the absence of CSB contributions proportional to  $c_{3,4}\delta m_N$  at order  $\nu = 5$ , see [21, 44]. It is easy to verify that terms in Eq. (3.24) proportional to  $\delta m_N$  are indeed reproduced in the  $\Delta$ -less theory by  $\Delta$ -saturation of the isospin-conserving sub-subleading pion-nucleon vertices (a complete list of these terms in the Lagrangian can be found in Ref. [45]) while the ones proportional to  $\delta m_\Delta^1$  and  $\delta m_\Delta^2$  arise from resonance saturation of the sub-subleading strong and electromagnetic isospin-breaking pion-nucleon vertices, see Fig.2.

To get a rough idea about the size of the isospin breaking 3NF contributions to e.g. the 3N binding energy, one can look at the strength of the corresponding  $r$ -space potentials in Eq. (3.25). For the CSC terms  $\propto \delta M_\pi^2$  one gets  $\delta M_\pi^2 g_A^2 h_A^2 M_\pi^4 / (144\pi^2 F_\pi^4 \Delta) \sim 50$  keV. Numerically, this is expected to be the biggest isospin-breaking 3NF effect. Notice that in the theory without explicit deltas, this contribution is shifted to the subleading order  $\nu = 5$  [21]. The strength of the remaining CSC 3NF contribution  $\propto \delta m_\Delta^2$  is much smaller,  $|\delta m_\Delta^2| g_A^2 h_A^2 M_\pi^6 / (384\pi^2 F_\pi^4 \Delta^2) \sim 1.5$  keV (here we use the central value for  $\delta m_\Delta^2 = -1.7$  MeV from Eq. (3.10)). The estimated size of the CSB 3NF in Eq. (3.25)

<sup>4</sup> Numerically, however, it is expected to give the strongest isospin-breaking 3NF [21], see also the discussion in the next paragraph.

using  $\delta m_{\Delta}^1 = -5.3$  MeV is

$$|\delta m_{\Delta}^1 - 3\delta m_N| \frac{g_A^2 h_A^2 M_{\pi}^6}{432\pi^2 F_{\pi}^4 \Delta^2} \sim 3 \text{ keV}, \quad (3.27)$$

which is comparable to the typical size of the leading CSB 3NF obtained in Ref. [21] and based on EFT without explicit deltas,  $\delta m_N g_A^4 M_{\pi}^4 / (256\pi^2 F_{\pi}^4) \sim 7$  keV. We further emphasize that the CSB 3NF in Eq. (3.24) vanishes exactly if one adopts the quark model relation (3.11).

### Acknowledgments

The work of E.E. and H.K. was supported in parts by funds provided from the Helmholtz Association to the young investigator group ‘‘Few-Nucleon Systems in Chiral Effective Field Theory’’ (grant VH-NG-222) and through the virtual institute ‘‘Spin and strong QCD’’ (grant VH-VI-231). This work was further supported by the DFG (SFB/TR 16 ‘‘Subnuclear Structure of Matter’’) and by the EU Integrated Infrastructure Initiative Hadron Physics Project under contract number RII3-CT-2004-506078.

- 
- [1] J.-I. Fujita and H. Miyazawa, *Prog. Theo. Phys.* **17**, 360 (1957).  
[2] B. H. J. McKellar and R. Rajaraman, *Phys. Rev. Lett.* **21**, 450 (1968).  
[3] S. A. Coon, M. D. Scadron and B. R. Barrett, *Nucl. Phys. A* **242**, 467 (1975).  
[4] H. T. Coelho *et al.*, *Phys. Rev. C* **28**, 1812 (1983).  
[5] B. S. Pudliner *et al.*, *Phys. Rev. C* **56**, 1720 (1997).  
[6] S. C. Pieper *et al.*, *Phys. Rev. C* **64**, 014001 (2001).  
[7] W. Glöckle *et al.*, *Phys. Rept.* **274**, 107 (1996).  
[8] N. Kalantar-Nayestanaki and E. Epelbaum, *Nucl. Phys. News* **17**, 22 (2007), [arXiv:nucl-th/0703089].  
[9] S. Weinberg, *Nucl. Phys.* **B363**, 3 (1991).  
[10] T. R. Hemmert, B. R. Holstein, and J. Kambor, *J. Phys. G* **24**, 1831 (1998), [arXiv:hep-ph/9712496].  
[11] H. Krebs, E. Epelbaum, and U.-G. Meißner, *Eur. Phys. J.* **A32**, 127 (2007), [arXiv:nucl-th/0703087].  
[12] B. C. Tiburzi and A. Walker-Loud, *Nucl. Phys. A* **764**, 274 (2006), [arXiv:hep-lat/0501018].  
[13] N. Fettes and U.-G. Meißner, *Nucl. Phys.* **A679**, 629 (2001), [arXiv:hep-ph/0006299].  
[14] U. van Kolck, *Phys. Rev.* **C49**, 2932 (1994).  
[15] E. Epelbaum, *Prog. Part. Nucl. Phys.* **57**, 654 (2006), [arXiv:nucl-th/0509032].  
[16] E. Epelbaum *et al.*, *Phys. Rev.* **C66**, 064001 (2002), [arXiv:nucl-th/0208023].  
[17] V. Bernard, N. Kaiser, and U.-G. Meißner, *Nucl. Phys.* **A615**, 483 (1997), [arXiv:hep-ph/9611253].  
[18] J. L. Friar, D. Huber, and U. van Kolck, *Phys. Rev.* **C59**, 53 (1999), [arXiv:nucl-th/9809065].  
[19] V. R. Pandharipande, D. R. Phillips, and U. van Kolck, *Phys. Rev.* **C71**, 064002 (2005), [arXiv:nucl-th/0501061].  
[20] E. Epelbaum and U.-G. Meißner, *Phys. Rev.* **C72**, 044001 (2005), [arXiv:nucl-th/0502052].  
[21] E. Epelbaum, U.-G. Meißner, and J. E. Palomar, *Phys. Rev.* **C71**, 024001 (2005), [arXiv:nucl-th/0407037].  
[22] J. L. Friar and U. van Kolck, *Phys. Rev.* **C60**, 034006 (1999), [arXiv:nucl-th/9906048].  
[23] J. L. Friar, U. van Kolck, G. L. Payne, and S. A. Coon, *Phys. Rev.* **C68**, 024003 (2003), [arXiv:nucl-th/0303058].  
[24] J. L. Friar, G. L. Payne, and U. van Kolck, *Phys. Rev.* **C71**, 024003 (2005), [arXiv:nucl-th/0408033].  
[25] J. L. Friar, U. van Kolck, M. C. M. Rentmeester, and R. G. E. Timmermans, *Phys. Rev.* **C70**, 044001 (2004), [arXiv:nucl-th/0406026].  
[26] R. Urech, *Nucl. Phys.* **B433**, 234 (1995), [arXiv:hep-ph/9405341].  
[27] U.-G. Meißner and S. Steininger, *Phys. Lett.* **B419**, 403 (1998), [arXiv:hep-ph/9709453].  
[28] G. Müller and U.-G. Meißner, *Nucl. Phys.* **B556**, 265 (1999), [arXiv:hep-ph/9903375].  
[29] J. Gasser, M. A. Ivanov, E. Lipartia, M. Mojžiš, and A. Rusetsky, *Eur. Phys. J.* **C26**, 13 (2002), [arXiv:hep-ph/0206068].  
[30] V. Bernard, T. R. Hemmert, and U.-G. Meißner, *Phys. Lett.* **B622**, 141 (2005), [arXiv:hep-lat/0503022].  
[31] V. Bernard, T. R. Hemmert, and U.-G. Meißner, *Nucl. Phys.* **A732**, 149 (2004), [arXiv:hep-ph/0307115].  
[32] H. R. Rubinstein, F. Scheck, and R. H. Sokolov, *Phys. Rev.* **154**, 1608 (1967).  
[33] Particle Data Group, see the website <http://pdg.lbl.gov/>.  
[34] A. B. Gridnev, I. Horn, W. J. Briscoe, and I. I. Strakovsky, *Phys. Atom. Nucl.* **69**, 1542 (2006), [arXiv:hep-ph/0408192].  
[35] V. V. Abaev and S. P. Kruglov, *Z. Phys.* **A352**, 85 (1995).  
[36] R. Koch and E. Pietarinen, *Nucl. Phys.* **A336**, 331 (1980).  
[37] E. Pedroni *et al.*, *Nucl. Phys.* **A300**, 321 (1978).

- [38] A. Bernicha, G. Lopez Castro, and J. Pestieau, Nucl. Phys. **A597**, 623 (1996), [arXiv:hep-ph/9508388].
- [39] R. A. Arndt, W. J. Briscoe, I. I. Strakovsky, and R. L. Workman, Phys. Rev. **C74**, 045205 (2006), [arXiv:nucl-th/0605082].
- [40] J. Gasser and H. Leutwyler, Phys. Rept. **87**, 77 (1982).
- [41] S. R. Beane, K. Orginos, and M. Savage, Nucl. Phys. **B768**, 38 (2007), [arXiv:hep-lat/0605014].
- [42] S. R. Coleman, J. Wess, and B. Zumino, Phys. Rev. **177**, 2239 (1969).
- [43] R. Haag, Phys. Rev. **112**, 669 (1958).
- [44] E. Epelbaum, AIP Conf. Proc. **768**, 174 (2005), [arXiv:nucl-th/0412003].
- [45] N. Fettes, U.-G. Meißner, and S. Steininger, Nucl. Phys. **A640**, 199 (1998), [arXiv:hep-ph/9803266].